# Gold(I) Macrocycles and [2]Catenanes Containing Sulfone-Functionalised Diacetylide Ligands

**Fabian Mohr,[a] Michael C. Jennings,[a] and Richard J. Puddephatt*[a]**

**Keywords:** Self assembly / Catenanes / Macrocycles / Gold / Aurophilicity

The reaction of the polymeric digold(I) diacetylide $[(AuCCCH_2OC_6H_4)_2SO_2]_n$ with diphosphane ligands PP leads to the formation of either macrocyclic ring complexes $[(AuCCCH_2OC_6H_4)_2SO_2(\mu\text{-PP})]$ or [2]catenanes $[(AuCCCH_2OC_6H_4)_2SO_2(\mu\text{-PP})]_2$ by a self-assembly process. With the diphosphane ligands $Ph_2PCCPPh_2$, $[Fe(C_5H_4PPh_2)_2]$ and $Ph_2P(CH_2)_nPPh_2$ ($n$ = 4, 5 and 6), macrocyclic ring complexes result, but with the diphosphane ligand $Ph_2P(CH_2)_3PPh_2$, the [2]catenane selectively crystallises from an isomeric mixture of products.
(© Wiley-VCH Verlag GmbH & Co. KGaA, 69451 Weinheim, Germany, 2003)

## Introduction

The promise of useful applications of nanoscale devices has stimulated intense research into the synthesis and properties of mechanically interlocked molecules such as catenanes and rotaxanes.[1−5] Synthetic strategies based on ideas such as π-π interactions, metal ion templation, hydrophobic forces and hydrogen bonding have been developed to assemble such supramolecular structures.[6,7] The vast majority of catenanes and rotaxanes prepared to date are based either on organic or inorganic molecules, and the first organometallic [2]catenane was reported only in 1993.[8]

Gold(I) has proven to be a versatile building-block for constructing organometallic network polymers, rings and catenanes because of the low steric effects associated with its tendency for linear coordination and the potential to form Au···Au aurophilic attractions that can enhance association between gold(I) centers.[9,10] These aurophilic attractions (bond energies of ca. 7−11 kcal mol$^{-1}$) result in gold−gold distances ranging from 2.75 to 3.40 Å.[11] Gold(I) is a labile metal center and so easy rearrangements can occur to give thermodynamic control of the self-assembly processes. Recently, the first detailed studies of organometallic [2]catenanes containing gold(I) centres and diacetylide bridging ligands have been reported.[12−15] This work has shown that both the "hinge group" (X) in the diacetylide ligand and the "spacer group" between the phosphorus atoms (Y) (Figure 1) determine whether [2]catenanes or macrocyclic complexes are formed. Short and sterically demanding spacer groups Y such as $(CH_2)_2$, HC=CH, C≡C and $[Fe(C_5H_4)_2]$ form macrocycles, whilst longer spacer groups such as $(CH_2)_4$ and $(CH_2)_5$ may form [2]catenanes, depending on the nature of the hinge group. The case where the spacer group is $(CH_2)_3$ represents the borderline between macrocycle and [2]catenane formation: mixtures of both structural forms are usually observed. The hinge group effect depends at least in part on the orientation of the aryl groups (the twist angles of the two aryl groups with respect to the plane of the hinge atom, Figure 2), with the combinations of angles approximating to 90, 45 or 45, 45 (found with X = $CH_2$, $CMe_2$ or CHAr) favouring [2]catenane formation, while the combination 90, 0 (found with X = O or S) is particularly unfavourable to [2]catenane formation and so leads to formation of the simple macrocycles only. The unfavourable combination of angles 90, 0 found with X = S arises from π-bonding between the sulfur atom and adjacent aryl groups. This $p_\pi$-$p_\pi$ bonding should not be present on oxidation of S to $SO_2$, and so catenation might then be possible. In order to study this potential method of triggering catenation, the selectivity of formation of [2]catenanes or macrocyclic rings with gold(I) bound to the sulfone-functionalized diacetylide and diphosphane ligands has been studied, and the results are presented below.

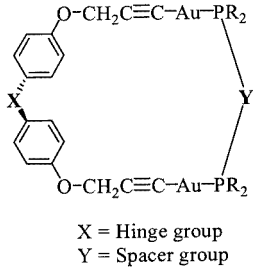


Figure 1. Schematic diagram of a macrocyclic gold(I) complex

[a] Department of Chemistry, University of Western Ontario, London, ON, N6A 5B7, Canada
Fax: (internat.) + 1-519/661-3022
E-mail: pudd@uwo.ca

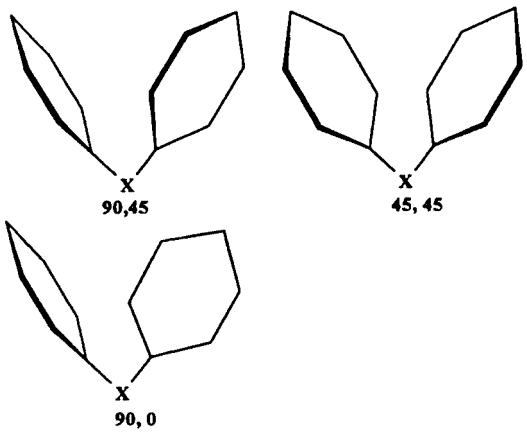


Figure 2. Orientation of aryl groups at the hinge atom X

## Results and Discussion

### Ligand and Gold(I) Oligomer Synthesis

Reaction of bis(4-hydroxyphenyl) sulfone with propargyl bromide under basic conditions gives the bis(alkyne) compound **1** (Scheme 1) in high yield. This was easily converted into the oligomeric digold(I) diacetylide complex **2** by reaction with [AuCl(SMe$_2$)] in the presence of triethylamine (Scheme 1). Complex **2** was isolated in high yield as a yellow powder, which was insoluble in common organic solvents. Like other gold(I) acetylides, it is presumed to have a polymeric structure in which each acetylide group is σ-bonded ($\eta^1$) to one gold atom and π-bonded ($\eta^2$) to another.[16] This is supported by the IR spectrum of **2**, which exhibits a weak band at 1996 cm$^{-1}$, considerably lower (133 cm$^{-1}$) than the corresponding band in the precursor **1** as would be expected if the alkynyl groups act as π donors.

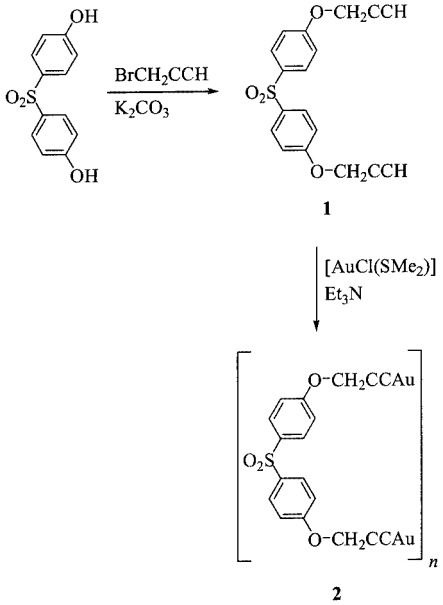


Scheme 1

### Reactions with Diphosphane Ligands

### Macrocyclic Ring Complexes

Reactions of complex **2** with a variety of diphosphane ligands gave colourless or pale-yellow, air-stable solids in good yields (Scheme 2). The new complexes were characterized by $^1$H and $^{31}$P NMR spectroscopy, MALDI-TOF mass spectrometry, elemental analyses and, in a number of cases, by X-ray crystallography. The $^{31}$P NMR spectra of the complexes show one singlet, with chemical shifts ranging from δ = 18.59 (**3a**) to 37.57 ppm (**3e**). The $^1$H NMR spectra show, in addition to the spacer group and $OCH_2$ resonances, two pairs of doublets at δ ≈ 7.8 and 7.1 ppm, corresponding to the protons on the *p*-disubstituted $SC_6H_4O$ rings. The simple $^1$H NMR spectra as well as the presence of only one singlet in the $^{31}$P NMR spectra show that these molecules have a high degree of symmetry and exist as single isomers in solution. The spectroscopic data are consistent with macrocyclic ring structures for the complexes containing the diphosphane ligands $Ph_2PCCPPh_2$ (**3a**), [Fe($C_5H_4PPh_2$)$_2$] (**3b**) and $Ph_2P(CH_2)_nPPh_2$ [*n* = 4 (**3c**), 5 (**3d**) and 6 (**3e**)]. The MALDI-TOF mass spectra show molecular ion peaks in each case, with no peak corresponding to the potential [2]catenane but this is not definitive evidence since the mechanical bond of a [2]catenane may be easily broken. The proposed macrocyclic structures of complexes **3a**, **3b** and **3d** have been confirmed crystallographically. Figures 3, 4, and 5 show the molecular structures, while selected bond lengths and angles are listed in Tables 1, 2, and 3.

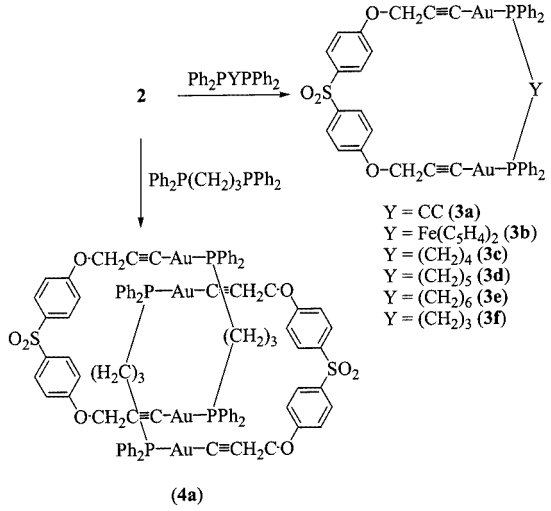


Scheme 2

The complexes consist of 23- (**3a**), 24- (**3b**) and 26-membered (**3d**) rings in which one diphosphane and one diacetylide ligand bridge two gold(I) centers. The angles C−Au−P are close to linearity in each case, as expected for gold(I). The molecular structures of the macrocyclic complexes are similar, but the three complexes pack very differently in the crystal space. Complex **3a** forms a polymeric

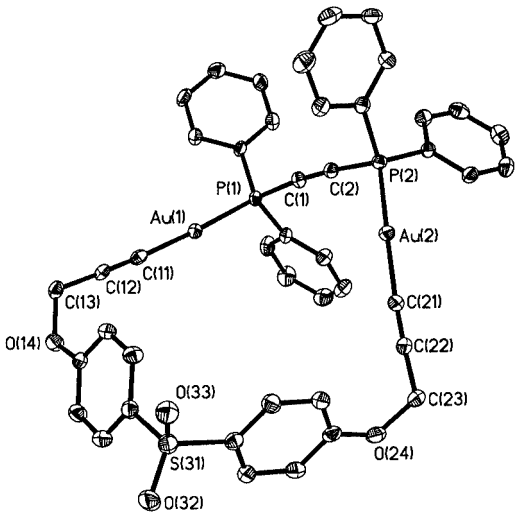


Figure 3. Molecular structure of complex **3a**; ellipsoids show 50% probability levels, hydrogen atoms have been omitted for clarity

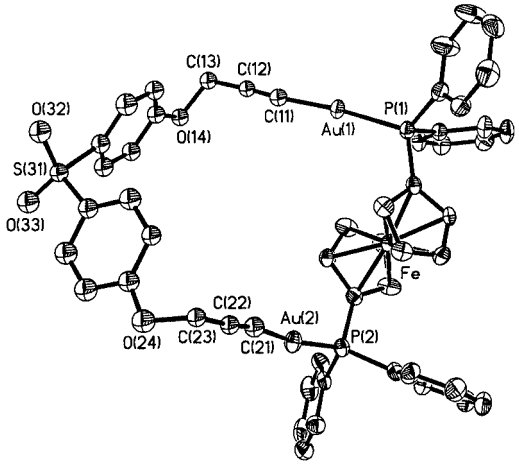


Figure 4. Molecular structure of complex **3b**; ellipsoids show 50% probability levels, hydrogen atoms have been omitted for clarity

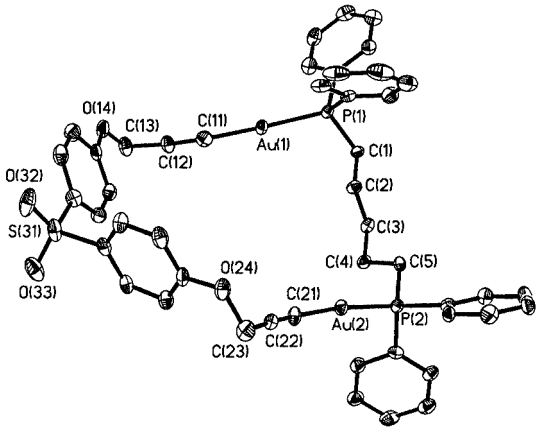


Figure 5. Molecular structure of complex **3d**; ellipsoids show 50% probability levels, hydrogen atoms have been omitted for clarity.

Table 1. Selected bond lengths [Å] and angles [°] in complex **3a**

| | | | |
|---|---|---|---|
| Au(1)−P(1) | 2.2709(18) | Au(2)−P(2) | 2.2749(15) |
| Au(1)−C(11) | 2.010(7) | Au(2)−C(21) | 2.008(6) |
| C(11)−C(12) | 1.192(9) | C(21)−C(22) | 1.201(8) |
| C(1)−C(2) | 1.212(8) | Au(1)···Au(2A) | 3.1819(3) |
| C(11)−Au(1)−P(1) | 176.27(17) | C(21)−Au(2)−P(2) | 171.85(19) |
| C(12)−C(11)−Au(1) | 176.1(6) | C(22)−C(21)−Au(2) | 176.0(6) |

Table 2. Selected bond lengths [Å] and angles [°] in complex **3b**

| | | | |
|---|---|---|---|
| Au(1)−P(1) | 2.2644(19) | Au(2)−P(2) | 2.2729(19) |
| Au(1)−C(11) | 1.968(18) | Au(2)−C(21) | 2.032(19) |
| C(11)−C(12) | 1.18(2) | C(21)−C(22) | 1.19(3) |
| | | Au(2)···Au(2A) | 3.1488(7) |
| C(11)−Au(1)−P(1) | 171.3(5) | C(21)−Au(2)−P(2) | 175.5(6) |
| C(12)−C(11)−Au(1) | 171.7(15) | C(22)−C(21)−Au(2) | 170.6(18) |

Table 3. Selected bond lengths [Å] and angles [°] in complex **3d**

| | | | |
|---|---|---|---|
| Au(1)−P(1) | 2.288(2) | Au(2)−P(2) | 2.276(2) |
| Au(1)−C(11) | 1.994(11) | Au(2)−C(21) | 1.984(8) |
| C(11)−C(12) | 1.233(13) | C(21)−C(22) | 1.208(11) |
| C(11)−Au(1)−P(1) | 178.0(3) | C(21)−Au(2)−P(2) | 171.0(3) |
| C(12)−C(11)−Au(1) | 176.5(9) | C(22)−C(21)−Au(2) | 168.3(8) |

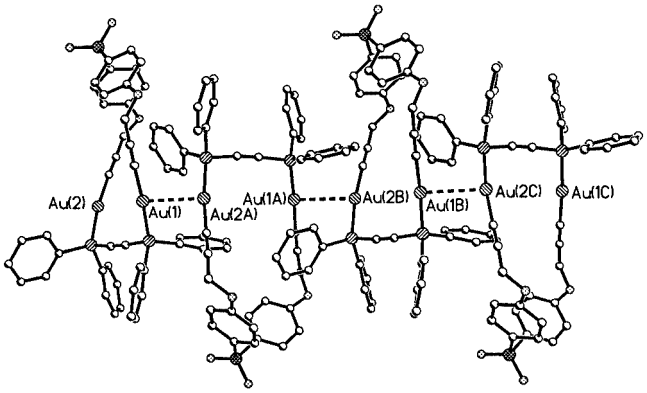


Figure 6. Packing of complex **3a** to form a polymeric chain

structure (Figure 6), resulting from aurophilic attractions [Au(1)···Au(2A) 3.1819(3) Å] between adjacent rings. Related polymers, formed by aurophilic attractions, are known with phosphane−gold(I) units in combination with halides, thiolates or acetylides.[9,11,17] In addition, the macrocycles in **3a** adopt an *anti* arrangement to minimise steric interactions. Macrocycle **3b** forms discrete dimeric units consisting of two rings connected by close gold−gold contacts [Au(2)···Au(2A) 3.1488(7) Å] (Figure 7), again the rings adopt an *anti* arrangement. In contrast, complex **3d** forms neither dimeric units nor a polymer: discrete macrocycles fill the crystal space.

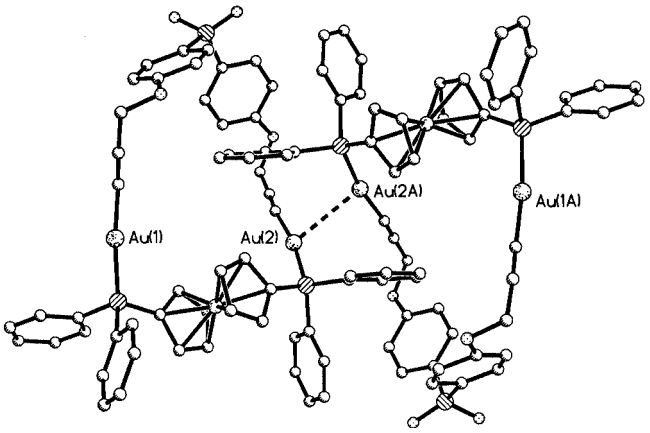


Figure 7. Packing of complex **3d** to form dimeric units

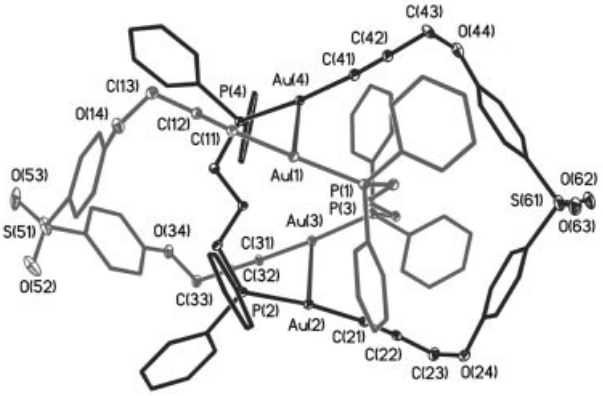


Figure 8. Molecular structure of complex **4a**; ellipsoids show 25% probability levels, $C_6H_4$ and phenyl rings are shown as lines and hydrogen atoms have been omitted for clarity

### *A [2]Catenane and Its Equilibrium with a Macrocycle*

Reaction of complex **2** with $Ph_2P(CH_2)_3PPh_2$ gives a colourless, air-stable solid (Scheme 2). The $^{31}P$ NMR spectrum of this product contained two major singlet resonances, and the $^1H$ NMR spectrum contained two major pairs of doublets for the $C_6H_4$ protons. There was also a third minor set of resonances. This indicates that the compound exists as a mixture of three isomers, as discussed previously for the complex $[Me_2C(C_6H_4OCH_2CC)_2Au_2(Ph_2PCH_2CH_2CH_2PPh_2)]$.[15] The two major isomers are assigned as the macrocyclic ring **3f** and the [2]catenane **4a** (Scheme 2). The [2]catenane is characterized by lower chemical shifts for the $C_6H_4$ protons (**4a**: $\delta$ = 6.16 and 7.30 ppm; **3f**: $\delta$ = 7.07 and 7.78 ppm) and for the phosphorus atoms (**4a**: $\delta$ = 31.47 ppm; **3f**: $\delta$ = 35.32 ppm). The proton shielding arises as a result of the rigid structure of the [2]catenane with close edge-to-face contact between the $C_6H_4$ groups and phenyl groups of the interlocked molecule, and is characteristic of the [2]catenane structure with $Ph_2P(CH_2)_3PPh_2$ ligands.[15] Curiously, single crystals of the pure [2]catenane **4a** were insoluble in common organic solvents. The MALDI-TOF mass spectrum of the crystals of **4a** does not show a molecular ion peak for the [2]catenane, but only a molecular ion peak for the simple macrocycle **3f**. Presumably the mechanical link is broken under the conditions used.

The structure of the [2]catenane **4a** is shown in Figure 8 and selected bond lengths and angles are listed in Table 4. The two macrocyclic rings are interlocked across the diphosphane ligand backbones. There are two close gold−gold contacts [Au(1)···Au(4) 3.2392(7) Å and Au(2)···Au(3) 3.3164(6) Å] and these aurophilic attractions no doubt favour the [2]catenane formation. In addition, there are several close phenyl−$C_6H_4$ and phenyl−phenyl interactions (Figure 8), and the sum of these secondary bonding energies is clearly enough to overcome the negative entropy associated with [2]catenane formation.

Table 4. Selected bond lengths [Å] and angles [°] in complex **4a**

| | | | |
|---|---|---|---|
| Au(1)−P(1) | 2.279(2) | Au(2)−P(2) | 2.275(3) |
| Au(3)−P(3) | 2.279(2) | Au(4)−P(4) | 2.273(2) |
| Au(1)···Au(4) | 3.2392(7) | Au(2)···Au(3) | 3.3164(6) |
| Au(1)−C(11) | 2.011(10) | Au(2)−C(21) | 1.998(10) |
| Au(3)−C(31) | 2.007(9) | Au(4)−C(41) | 1.996(10) |
| C(11)−C(12) | 1.181(12) | C(21)−C(22) | 1.220(13) |
| C(31)−C(32) | 1.192(12) | C(41)−C(42) | 1.193(14) |
| C(11)−Au(1)−P(1) | 172.1(3) | C(21)−Au(2)−P(2) | 172.9(3) |
| C(31)−Au(3)−P(3) | 171.7(3) | C(41)−Au(4)−P(4) | 170.4(4) |

## Conclusion

It is shown that the reaction of the sulfone-functionalised polymeric dialkynyldigold(I) complex **2** (Scheme 1) with diphosphane ligands can lead to the self-assembly of macrocyclic rings or of a [2]catenane, depending on the nature of the spacer group in the diphosphane ligand. Short or bulky spacer groups form macrocyclic rings, because the ring cavity is too small to allow interlocking to form the [2]catenane. A [2]catenane is formed, in equilibrium with the macrocyclic complex, with the intermediate-length $(CH_2)_3$ spacer group. A macrocycle is formed with the longer $(CH_2)_5$ spacer group and, probably, also with the $(CH_2)_4$ spacer group. The aim of this work was to study the influence of the sulfone unit as a "hinge group" X (Figure 1), in supporting [2]catenane formation. Compared to the hinge groups studied previously, it is clear that the $SO_2$ group is better than X = S or O, but not so good as X = $CH_2$, $CMe_2$, $C_6H_{10}$ (cyclohexylidene) or $CH(C_6H_4Br)$ for promoting formation of [2]catenanes. Thus, when X = S or O, no [2]catenane is detected in any case, whereas the carbon-based hinge groups give catenanes when the diphosphane is $Ph_2P(CH_2)_nPPh_2$, with $n$ = 3−5.[12−15] Some key structural parameters are listed in Table 5. The hinge angles are not greatly distorted from the ideal tetrahedral angles and are slightly more open than for the sulfide hinge group (Table 5). The aryl groups in all complexes studied are twisted out of the plane defined by the C−S−C group with angles between the 90, 90° and 90, 45° combinations that are favourable for [2]catenane formation and very different from the case with X = S (Table 5). It is therefore not obvious why [2]catenane formation is less favoured when X = $SO_2$ than when X = $CH_2$ or $CMe_2$ (Table 5). The differ-

Table 5. The hinge angles and aryl twist angles [°] for selected complexes

| Hinge group X | Spacer group Y | Hinge angle | Aryl twists | Structure |
|---|---|---|---|---|
| $SO_2$ | CC | 104.7(3) | 100, 100 | ring |
| $SO_2$ | $Fe(C_5H_4)_2$ | 109.4(7) | 97(95), 87(43)[a] | ring |
| $SO_2$ | $(CH_2)_5$ | 105.9(4) | 95, 65 | ring |
| $SO_2$ | $(CH_2)_3$ | 105.4(5)/ 107.9(5) | 89, 69/87, 71[b] | catenane |
| S | $(CH_2)_4$ | 104.3(3) | 97, 1 | ring |
| $CH_2$ | $(CH_2)_4$ | 115.0(6)/115.3(5) | 92, 33/93, 29 [b] | catenane |
| $CMe_2$ | $(CH_2)_4$ | 111.2(7)/111.9(9) | 52, 47/49, 39 [b] | catenane |

[a] Two values because of structural disorder. [b] Two values for two independent rings.

ences could be caused by subtle differences in hinge angles, or by electronic effects of the hinge groups on the strengths of phenyl−aryl attractions. Nevertheless, the comparison of the hinge groups S and $SO_2$ does show how the orientation of the aryl groups can be controlled and the effect could in principle be used to trigger catenation on oxidation of S to $SO_2$. Our attempts to demonstrate the effect directly have been unsuccessful since the Au−C bonds are not stable to strongly oxidising conditions.

## Experimental Section

**General Remarks:** NMR spectra were recorded using Varian Mercury 400 and Inova 600 MHz spectrometers. $^1H$ and $^{13}C$ NMR chemical shifts are reported relative to tetramethylsilane, while $^{31}P$ NMR chemical shifts are reported relative to 85% $H_3PO_4$ as an external standard. IR spectra were recorded using a Perkin−Elmer 2000 FT-IR as Nujol mulls on NaCl plates. MALDI-TOF spectra were recorded using a Micromass MALDI-LR instrument in positive ion mode. The samples were dissolved in $CH_2Cl_2$ and spotted onto a dried layer of matrix [1 μL of α-cyano-4-hydroxycinnamic acid (10 mg/mL in CAN/EtOH, 50:50)]. The samples were analysed in reflection mode and mass spectra were externally calibrated using a tryptic digest of alcohol dehydrogenase. The complex [AuCl(SMe$_2$)] was prepared by a literature procedure.[18] All other chemicals and solvents were from commercial sources and used as received. All reactions involving gold complexes were carried out in reactions vessels shielded from light. Elemental analyses were carried out by Guelph Chemical Laboratories, Guelph, Canada.

**Diacetylide Ligand 1**: $BrCH_2C{\equiv}CH$ (2.4 g, 17.58 mmol) and $K_2CO_3$ (1.6 g, 11.58 mmol) were added to a solution of $O_2S(4\text{-}C_6H_4OH)_2$ (2.0 g, 7.99 mmol) in acetone (50 mL). The mixture was heated under reflux for about 24 h. The cooled solution was filtered to give a pale yellow filtrate. The solvent was removed under reduced pressure and the resultant off-white solid dried under vacuum. Yield: 2.3 g, 88%. IR (nujol): $\tilde{\nu}$ = 2080 (br, w) 2129 $cm^{-1}$ (s) (C≡C). $^1H$ NMR (400 MHz, [D$_6$]acetone, 25 °C): δ = 7.91 (d, $J$ = 9.4 Hz, 4 H, $C_6H_4$), 7.16 (d, $J$ = 8.6 Hz, 4 H, $C_6H_4$), 4.89 (d, $J$ = 2.4 Hz, 2 H, $OCH_2$), 3.14 (t, $J$ = 2.4 Hz, 2 H, C≡H) ppm. $^{13}C$ NMR (100 MHz, [D$_6$]acetone, 25 °C): δ = 161.2, 135.2, 129.6, 115.6 (all $C_6H_4$), 78.2 (C≡CH), 77.2 (C≡*C*H), 56.2 ($OCH_2$) ppm. MS: *m*/*z* (%) = 326 (72) $[M]^+$. $C_{18}H_{14}O_4S$ (326.4): calcd. C 66.24, H .32; found C 65.79, H 4.57.

**Digold(I) Diacetylide 2**: [AuCl(SMe$_2$)] (0.452 g, 1.53 mmol) was dissolved in THF (50 mL)/MeOH (30 mL). A solution of **1** (0.250 g, 0.77 mmol) and $Et_3N$ (0.4 mL, 2.87 mmol) in THF (20 mL)/MeOH (10 mL) was added to this. The resulting mixture was stirred for 3 h to produce a yellow precipitate. The solid was then collected by filtration, washed with THF, MeOH, $Et_2O$ and pentane, and dried. Yield: 0.499 g, 91%. The product was insoluble in common organic solvents. IR (nujol): $\tilde{\nu}$ = 1996 $cm^{-1}$ (w) (C≡C). $C_{18}H_{12}Au_2O_4S$ (718.3): calcd. C 30.10, H 1.68; found C 30.56, H 1.92.

**Macrocycle 3a**: A mixture of **2** (0.100 g, 0.139 mmol) and $Ph_2PCCPPh_2$ (0.044 g, 0.112 mmol) in $CH_2Cl_2$ (10 mL) was stirred for 3 h at room temperature. The mixture was filtered through Celite and the filtrate concentrated under vacuum (ca. 2−3 mL). Addition of $Et_2O$ precipitated an off-white solid. The powder was collected by filtration, washed with $Et_2O$ and pentane, and dried. Yield 0.078 g, 51%. $^{31}P$ NMR (162 MHz, $CDCl_3$, 25 °C): δ = 18.59 ppm. $^1H$ NMR (400 MHz, $CDCl_3$, 25 °C): δ = 7.86 (d, $J$ = 7.9 Hz, 4 H, $C_6H_4$), 7.62−7.69 (m, 8 H, Ph), 7.52−7.58 (m, 4 H, Ph), 7.43−7.49 (m, 8 H, Ph), 7.13 (d, $J$ = 9.3 Hz, 4 H, $C_6H_4$), 4.91 (s, 4 H, $OCH_2$) ppm. MALDI-TOF MS: *m*/*z* (%) = 1113 (19) $[MH]^+$. $C_{44}H_{32}Au_2O_4PS{\cdot}1/2Et_2O$ (1149.7): calcd. C 48.05, H 3.24; found C 48.86, H 2.92. Crystals suitable for X-ray diffraction were grown by slow diffusion of hexane into a concentrated $CH_2Cl_2$ solution.

**Macrocycle 3b**: This was prepared by the procedure described for **3a** from **2** (0.075 g, 0.104 mmol) and [Fe($C_5H_4PPh_2$)$_2$] (0.046 g, 0.083 mmol). The product was isolated as a pale-yellow solid. Yield 0.097 g, 74%. $^{31}P$ NMR (162 MHz, $CDCl_3$, 25 °C): δ = 36.79 ppm. $^1H$ NMR (400 MHz, $CDCl_3$, 25 °C): δ = 7.87 (d, $J$ = 8.6 Hz, 4 H, $C_6H_4$), 7.36−7.51 (m, 20 H, Ph), 7.16 (d, $J$ = 9.3 Hz, 4 H, $C_6H_4$), 4.94 (s, 4 H, $OCH_2$), 4.33 (s, 4 H, $C_5H_4$), 4.27 (s, 4 H, $C_5H_4$) ppm. MALDI-TOF MS: *m*/*z* (%) = 1273 (100) $[MH]^+$. $C_{52}H_{40}Au_2FeO_4P_2S{\cdot}0.2CH_2Cl_2$ (1289.7): calcd. C 48.50, H 3.15; found C 48.54, H 3.18. Crystals suitable for X-ray diffraction were grown by slow diffusion of $Et_2O$ into a concentrated nitrobenzene solution.

**Macrocycle 3c**: This was prepared by the procedure described for **3a** from **2** (0.100 g, 0.139 mmol) and $Ph_2P(CH_2)_4PPh_2$ (0.113 g, 0.083 mmol). The product was isolated as a colourless solid. Yield 0.110 g, 71%. $^{31}P$ NMR (162 MHz, $CDCl_3$, 25 °C): δ = 38.27 ppm. $^1H$ NMR (400 MHz, $CDCl_3$, 25 °C): δ = 7.85 (d, $J$ = 8.6 Hz, 4 H, $C_6H_4$), 7.60−7.38 (m, 20 H, Ph), 7.15 (d, $J$ = 8.6 Hz, 4 H, $C_6H_4$), 4.90 (s, 4 H, $OCH_2$), 2.27 (m, 4 H, $CH_2$), 1.65 (m, 4 H, $CH_2$) ppm. MALDI-TOF MS: *m*/*z* (%) = 1144 (100) $[MH]^+$. $C_{46}H_{40}Au_2O_4P_2S$ (1144.8): calcd. C 48.26, H 3.52; found C 48.16, H 3.75.

**Macrocycle 3d** This was prepared by the procedure described for **3a** from **2** (0.100 g, 0.139 mmol) and $Ph_2P(CH_2)_5PPh_2$ (0.052 g, 0.118 mmol). The product was isolated as a cream-coloured solid. Yield 0.126 g, 80%. $^{31}P$ NMR (162 MHz, $CDCl_3$, 25 °C): δ = 37.06 ppm. $^1H$ NMR (400 MHz, $CDCl_3$, 25 °C): δ = 7.87 (d, $J$ = 8.6 Hz, 4 H, $C_6H_4$), 7.54−7.62 (m, 8 H, Ph), 7.39−7.51 (m, 12 H, Ph), 7.16 (d, $J$ = 8.6 Hz, 4 H, $C_6H_4$), 4.95 (s, 4 H, $OCH_2$), 2.29 (m, 4 H,

$CH_2$), 1.50 (m, 6 H, $CH_2$) ppm. MALDI-TOF MS: *m/z* (%) = 1159 (100) $[MH]^+$. $C_{47}H_{42}Au_2O_4P_2S{\cdot}1/2CH_2Cl_2$ (1201.2): calcd. C 47.49, H 3.61; found C 47.62, H 3.70. Crystals suitable for X-ray diffraction were grown by slow diffusion of hexane into a concentrated $CH_2Cl_2$ solution.

**Macrocycle 3e:** This was prepared by the procedure described for **3a** from **2** (0.075 g, 0.104 mmol) and $Ph_2P(CH_2)_6PPh_2$ (0.038 g, 0.084 mmol). The product was isolated as a colourless solid. Yield 0.073 g, 61%. $^{31}P$ NMR (162 MHz, $CDCl_3$, 25 °C): δ = 37.57 ppm. $^1H$ NMR (400 MHz, $CDCl_3$, 25 °C): δ = 7.83 (d, *J* = 8.6 Hz, 4 H, $C_6H_4$), 7.37−7.65 (m, 20 H, Ph), 7.09 (d, *J* = 9.3 Hz, 4 H, $C_6H_4$), 4.84 (s, 4 H, $OCH_2$), 2.31, 1.51, 1.36 (m, 4 H, $CH_2$) ppm. MALDI-TOF MS: *m/z* (%) = 1173 (100) $[MH]^+$. $C_{48}H_{44}Au_2O_4P_2S{\cdot}CH_2Cl_2{\cdot}Et_2O$ (2502.7): calcd. C 48.47, H 3.95; found C 48.58, H 3.79.

**Macrocycle 3f and [2]Catenane 4a:** This was prepared as an equilibrium mixture by the procedure described for **3a** from **2** (0.075 g, 0.104 mmol) and $Ph_2P(CH_2)_3PPh_2$ (0.035 g, 0.085 mmol). The product was isolated as a colourless solid. Yield 0.093 g, 80%. **3f**: $^{31}P$ NMR (162 MHz, $CDCl_3$, 25 °C): δ = 35.32 ppm. $^1H$ NMR (600 MHz, $CDCl_3$, 25 °C): δ = 7.78 (d, *J* = 9 Hz, 4 H, $C_6H_4$), 7.36−7.51 (m, 20 H, Ph), 7.07 (d, *J* = 9 Hz, 4 H, $C_6H_4$), 4.95 (s, 4 H, $OCH_2$), 2.42 (m, 8 H, $CH_2$), 1.78 (m, 4 H, $CH_2$). **4a**: $^{31}P$ NMR (162 MHz, $CDCl_3$, 25 °C): δ = 31.47 ppm. $^1H$ NMR (600 MHz, $CDCl_3$, 25 °C): δ = 7.30 (d, *J* = 9 Hz, 4 H, $C_6H_4$), 7.36−7.51 (m, 20 H, Ph), 6.16 (d, *J* = 9 Hz, 4 H, $C_6H_4$), 4.94 (s, 4 H, $OCH_2$), 2.73 (m, 8 H, $CH_2$), 1.82 (m, 4 H, $CH_2$) ppm. MALDI-TOF MS: *m/z* (%) = 1131 (100) $[M/2 + H]^+$. $C_{90}H_{76}Au_4O_8P_4S_2$ (2261.5): calcd. C 47.80, H 3.39; found C 47.47, H 3.62. Crystals of **4a** suitable for X-ray diffraction were grown by slow diffusion of hexane into a concentrated $CH_2Cl_2$ solution.

**X-ray Crystallographic Study:** Data for **3a**, **3b**, **3d** and **4a** were collected at −73 °C by using a Nonius Kappa CCD diffractometer operating with Mo-$K_\alpha$ radiation (graphite monochromator, λ = 0.7107 Å) using COLLECT software.[19] The unit cell parameters were calculated and refined from the full data set. Crystal cell refinement and data reduction was carried out using DENZO and absorption correction was carried out using SCALEPACK.[20] The structures were solved by direct methods[21] (**3a**, **3b** and **4a**) or Patterson methods[22] (**3d**) and were refined using Fourier techniques.[23] Hydrogen atoms were included at geometrically determined positions riding on their respective carbon atoms. The atomic scattering factors were taken from standard sources.[24,25] All calculations were performed using the SHELXTL 5.1 program package.[26] Table 6 summarises the crystallographic and refinement details for all complexes. CCDC-185297 (**3a**), -185298 (**3b**), -185299 (**3d**) and -185300 (**4a**) contain the supplementary crystallographic data for this paper. These data can be obtained free of charge at www.ccdc.cam.ac.uk/conts/retrieving.html or from the Cambridge Crystallographic Data Centre, 12, Union Road, Cambridge CB2 1EZ, UK [Fax: (internat.) + 44-1223/336-033; E-mail: deposit@ccdc.cam.ac.uk].

**3a**: A colourless needle of $[(\mu\text{-}Ph_2PCCPPh_2)Au_2(\mu\text{-}CCCH_2\text{-}OC_6H_4S(O)_2C_6H_4OCH_2CC)]{\cdot}3CH_2Cl_2$ was mounted on a glass fibre. All of the non-hydrogen atoms were refined with anisotropic thermal parameters. One of the three occluded solvent molecules showed some occupational disorder. All three solvent molecules were refined with the bond lengths fixed (C−Cl = 1.65 Å and Cl···Cl = 2.74 Å). Solvent molecule one (C41) and two (C51) were refined anisotropically. The third solvent molecule (C61) was refined isotropically as a 70:30 disorder. The hydrogen atoms were included for all solvent molecules.

Table 6. Crystal and refinement data for complexes **3a**, **3b**, **3d** and **4a**

| | **3a** | **3b** | **3d** | **4a** |
|---|---|---|---|---|
| Empirical formula | $C_{47}H_{38}Au_2Cl_6O_4P_2S$ | $C_{59}H_{52.5}Au_2N_{0.5}O_6P_2S$ | $C_{49.75}H_{47.50}Au_2Cl_{5.50}O_4P_2S$ | $C_{92}H_{81}Au_4Cl_4O_8P_4S_2$ |
| Formula mass | 1367.41 | 1408.30 | 1392.29 | 2432.23 |
| Crystal size [mm] | 0.40 × 0.10 × 0.08 | 0.10 × 0.10 × 0.04 | 0.46 × 0.10 × 0.03 | 0.30 × 0.18 × 0.10 |
| *T* [K] | 200(2) | 200(2) | 200(2) | 200(2) |
| Crystal system | monoclinic | monoclinic | triclinic | monoclinic |
| Space group | $P2_1/c$ | $C2/c$ | $P\bar{1}$ | $P2_1/n$ |
| *a* [Å] | 16.5607(2) | 33.0021(4) | 14.1532(3) | 12.56950(10) |
| *b* [Å] | 13.8361(2) | 15.6311(2) | 14.4715(4) | 22.4692(3) |
| *c* [Å] | 22.9485(4) | 22.1400(3) | 14.6846(4) | 31.4742(4) |
| α [°] | 90 | 90 | 72.9000(10) | 90 |
| β [°] | 111.0280(10) | 97.756(7) | 67.81130(10) | 97.9920(10) |
| γ [°] | 90 | 90 | 73.7070(10) | 90 |
| *V* [Å$^3$] | 4908.14(13) | 11316.6(3) | 2612.58(12) | 8802.81(18) |
| Z | 4 | 8 | 2 | 4 |
| $\rho_{calcd.}$ [g cm$^{-1}$] | 1.851 | 1.653 | 1.770 | 1.835 |
| μ [mm$^{-1}$] | 6.448 | 5.568 | 6.033 | 6.943 |
| *F*(000) | 2632 | 5504 | 1351 | 4692 |
| Absorption correction | integration | integration | integration | integration |
| Transmission range | 0.6434−0.1824 | 0.8080−0.6059 | 0.8397−0.1678 | 0.5436−0.2299 |
| θ limits [°] | 2.64/27.60 | 2.55/27.50 | 2.73/27.50 | 2.59/27.49 |
| Measured reflections | 49456 | 83894 | 23715 | 59691 |
| Unique reflections | 11314 ($R_{int}$ = 0.055) | 12954 ($R_{int}$ = 0.091) | 11886 ($R_{int}$ = 0.090) | 19849 ($R_{int}$ = 0.068) |
| Parameters | 503 | 475 | 535 | 931 |
| GOF on $F^2$ | 1.055 | 1.025 | 1.019 | 1.202 |
| *R*1 [$I > 2\sigma(I)$] | 0.0420 | 0.0518 | 0.0605 | 0.0595 |
| *wR*2 (on $F^2$, all data) | 0.1136 | 0.1460 | 0.1686 | 0.1288 |
| $\Delta\rho_{min/max}$ [e Å$^{-3}$] | 2.579/−2.242 | 1.867/−0.751 | 2.744/−1.677 | 1.678/−1.224 |

**3b**: A yellow-orange diamond plate of [μ-[Fe($C_5H_4PPh_2$)$_2$]Au$_2$(μ-$CCH_2OC_6H_4S(O)_2C_6H_4OCH_2CC$)]·1/2$PhNO_2$·$Et_2O$ was mounted on a glass fibre. The $SO_2$ bridging ligand was disordered. It was modeled as a mixture of two isotropic moieties (60:40). All of the remaining non-hydrogen atoms were refined with anisotropic thermal parameters. The nitrobenzene was modeled at a half occupancy and the ether at full occupancy. Both solvent molecules were kept isotropic.

**3d**: A colourless plate of [(μ-$Ph_2P(CH_2)_5PPh_2$)Au$_2$(μ-$CCCH_2OC_6H_4S(O)_2C_6H_4OCH_2CC$)]·2.75$CH_2Cl_2$ was mounted on a glass fibre. All of the non-hydrogen atoms were refined with anisotropic thermal parameters. The solvent molecules showed some disorder. One solvent molecule (C41) was refined anisotropically. The second solvent molecule (C51) was refined at 75% occupancy with the bond lengths fixed as above. The third solvent molecule (C61) was refined isotropically as a 70:30 disorder, with fixed bond lengths. The hydrogen atoms were included for all solvent molecules.

**4a**: A colourless crystal of [(μ-$Ph_2P(CH_2)_3PPh_2$)Au$_2$(μ-$CCCH_2OC_6H_4S(O)_2C_6H_4OCH_2CC$)]$_2$·2$CH_2Cl_2$ was mounted on a glass fibre. All of the non-hydrogen atoms were refined with anisotropic thermal parameters. The two solvent molecules were refined anisotropically, with hydrogen atoms included and with bond lengths fixed as above.

## Acknowledgments

We thank the National Science and Engineering Research Council (Canada) for financial support. R. J. P. thanks the Government of Canada for a Canada Research Chair.

[1] *Molecular Catenanes, Rotaxanes and Knots* (Eds.: J.-P. Sauvage, C. Dietrich-Buchecker), Wiley-VCH, Weinheim, **1999**.
[2] M. Fujita, *Acc. Chem. Res.* **1999**, *32*, 53−61.
[3] A. R. Pease, J. O. Jeppesen, J. F. Stoddart, Y. Lio, C. P. Collier, J. R. Heath, *Acc. Chem. Res.* **2001**, *34*, 433−444.
[4] G. F. Swiegers, T. J. Malefetse, *Chem. Rev.* **2000**, *100*, 3483−3573.
[5] V. Balzani, A. Credi, F. M. Raymo, J. F. Stoddart, *Angew. Chem.* **2000**, *112*, 3484−3530; *Angew. Chem. Int. Ed.* **2000**, *39*, 3348−3391.
[6] S. Leininger, B. Olenyuk, P. J. Stang, *Chem. Rev.* **2000**, *100*, 853−908.
[7] G. Schill, *Catenanes, Rotaxanes and Knots*, Academic Press, New York, **1971**.
[8] G.-J. M. Gruter, F. J. J. de Kanter, P. R. Markies, T. Nomoto, O. S. Akkerman, F. Bickelhaupt, *J. Am. Chem. Soc.* **1993**, *115*, 12179−12180.
[9] R. J. Puddephatt, *Coord. Chem. Rev.* **2001**, *216−217*, 313−332.
[10] R. J. Puddephatt, *Chem. Commun.* **1998**, 1055−1062.
[11] H. Schmidbaur, *Chem. Soc. Rev.* **1995**, *24*, 391−400.
[12] C. P. McArdle, M. C. Irwin, M. C. Jennings, R. J. Puddephatt, *Angew. Chem. Int. Edn. Engl.* **1999**, *38*, 3376−3378.
[13] C. P. McArdle, J. J. Vittal, R. J. Puddephatt, *Angew. Chem. Int. Ed.* **2000**, *39*, 3819−3822.
[14] C. P. McArdle, M. C. Jennings, J. J. Vittal, R. J. Puddephatt, *Chem. Eur. J.* **2001**, *7*, 3572−3583.
[15] C. P. McArdle, M. C. Irwin, M. C. Jennings, J. J. Vittal, R. J. Puddephatt, *Chem. Eur. J.* **2002**, *8*, 723−734.
[16] D. M. P. Mingos, J. Yau, S. Menzer, D. J. Williams, *Angew. Chem. Int. Edn.* **1995**, *34*, 1894−1895.
[17] P.M. van Calcar, M.M. Olmstead, A.L. Balch, *Inorg. Chem.* **1997**, *36*, 5231−5238.
[18] A. Tamaki, J. K. Kochi, *J. Organomet. Chem.* **1974**, *64*, 411−425.
[19] *COLLECT, data collection software*, Nonius BV, **1999**.
[20] Z. Otwinowski, W. Minor in *Methods in Enzymology* (Ed.: R. M. Sweet), Academic Press, New York, **1997**.
[21] A. Altomare, M. Cascarano, C. Giacovazzo, A. Guagliardi, M. C. Burla, G. Polidori, M. Camalli, *J. Appl. Crystallogr.* **1994**, *27*, 1045−1050.
[22] P. T. Beurskens, G. Admiraal, G. Beurskens, W. P. Bosman, S. Garcia-Granda, R. O. Gould, J. M. M. Smits, C. Smykalla, *PATTY: The DIRDIF Program System*, Technical Report of the Crystallography Laboratory; University of Nijmegen, **1992**.
[23] P. T. Beurskens, G. Admiraal, G. Beurskens, W. P. Bosman, R. de Gelder, R. Israel, J. M. M. Smits, *The DIRDIF-94 Program System, Technical Report of the Crystallography Laboratory; University of Nijmegen*, **1994**.
[24] D. T. Cromer, J. T. Waber, *International Tables for X-ray Crystallography*, Kynoch Press, Birmingham, England, **1974**.
[25] *International Tables for Crystallography*, Kluwer Academic, Dordrecht, The Netherlands, **1992**.
[26] G. M. Sheldrick, *SHELXTL 5.1*, Universität Göttingen, **1998**.
Received August 30, 2002
[I02491]